Data-Driven Extension of "Measurement-Based Fast Coordinated Voltage Control for Transmission Grids"

Zhiyuan Tang, *Member, IEEE,* Etinosa Ekomwenrenren, *Student Member, IEEE,*
John W. Simpson-Porco, *Member, IEEE,* Evangelos Farantatos, *Senior Member, IEEE,*
Mahendra Patel, *Fellow, IEEE,* and Aboutaleb Haddadi, *Senior Member, IEEE,*

***Abstract*—In [1] a measurement-based coordinated voltage controller for transmission systems was developed. As essential model information, the controller incorporates linear sensitivities between device set-points and voltages/power injections in the grid. This letter details how online sensitivity estimation using robust least squares can be used in place of model-based sensitivities, leading to a model-free voltage control approach.**

***Index Terms*—Voltage control, measurement-based, transmission grid, model-free**

I. Introduction

In [1] the authors developed a measurement-based coordinated voltage control scheme for the next generation transmission grid with modern wide-area measurement and communication infrastructure. The controller coordinates synchronous generators (SGs), static var compensators (SVCs), and inverter-based resources (IBRs) in a systematic and automatic feedback manner to maintain bus voltages within limits in the presence of unmeasured disturbances. The controller is straightforward to implement, computationally very simple, applicable to large-scale power systems, and was extensively validated via simulation. The only required system model information is an approximate steady-state sensitivity model of the grid [1], relating changes in device set-points (e.g., AVR set-points) to measured variables (e.g., bus voltages).

In the design of [1], the sensitivity model is computed offline, based on the network bus admittance matrix and on the current dispatch point. However, this offline sensitivity model may be inaccurate compared to the true sensitivity in the system at a given moment. This may occur due to operating point drift, or more significantly, after grid topology changes due to line trips. Although the controller in [1] is designed to ensure closed-loop stability despite inaccuracies in the sensitivity model, as demonstrated in Scenario 2 of our case study, inaccuracy of the sensitivity model will lead to inefficient use of voltage control resources and even unsuccessful handling of voltage violations.

Our main contribution in this letter is to augment the control scheme in [1] with a fast robust sensitivity-estimation algorithm. This estimation block is decoupled from the voltage controller block proposed in [1], and uses the same high-resolution time-synchronized PMU measurements used in the controller to continuously re-estimate the required sensitivity information in real-time. Such a modular extension leads to a model-free voltage control design which adapts to real-time system conditions. In the literature, several regression methods have been used to estimate linearized power system models; see, e.g., [2], [3] and references therein. However, as shown in Fig. 4, some of these methods are sensitive to outliers in the data collected during system dynamic transients after contingencies occur (here, "outliers" refers both to measurement errors and to measurements that do not follow the quasi steady-state sensitivity relationship described in (1)). To ensure reliable online operation, here we specifically adopt a robust multivariate regression method and apply it in a recursive manner. To our knowledge, this method has not been utilized in the power system domain before. To further reduce the computational burden of this estimation, an event-triggered implementation is also discussed. We illustrate our method via various case studies on a detailed 9-bus system model.

II. Robust Estimation of Sensitivity Model

A. Problem Formulation

The sensitivity model employed in [1] can be described at the sampling instants by the following discrete-time model:

$$\Delta \boldsymbol{y}^k = \boldsymbol{\Pi}^k \Delta \boldsymbol{u}^k \tag{1}$$

where vectors $\Delta \boldsymbol{y}^k = \boldsymbol{y}^k - \boldsymbol{y}^{k-1} \in \mathbb{R}^n$ and $\Delta \boldsymbol{u} = \boldsymbol{u}^k - \boldsymbol{u}^{k-1} \in \mathbb{R}^m$ denote the changes in the measured outputs and control inputs, respectively; the matrix $\boldsymbol{\Pi}^k \in \mathbb{R}^{n\times m}$ is the sensitivity matrix. While $\boldsymbol{\Pi}^k$ is regarded as constant in [1], it will be updated online in this letter to adapt to changing system conditions. Specifically, our goal is to estimate the sensitivity matrix $\boldsymbol{\Pi}^k$ in (1) via the latest h measurement samples of the variables $\Delta \boldsymbol{u}$ and $\Delta \boldsymbol{y}$. For notational convenience, we let $\boldsymbol{Z}^k = [\boldsymbol{U}^k, \boldsymbol{Y}^k] \in \mathbb{R}^{h\times(n+m)}$ denote the set of available data, where $\boldsymbol{U}^k = [\Delta \boldsymbol{u}^{k-h+1}, \ldots, \Delta \boldsymbol{u}^k]^\top \in \mathbb{R}^{h\times m}$ and

Z. Tang is with the School of Electrical Engineering, Sichuan University, Chengdu 610065, China (e-mail: tangzhiyuan@scu.edu.cn).

E. Ekomwenrenren is with the Department of Electrical and Computer Engineering, University of Waterloo, Waterloo, ON N3L 3G1 CA (e-mail: etinosa.ekomwenrenren@uwaterloo.ca).

J. W. Simpson-Porco is with the Department of Electrical and Computer Engineering, University of Toronto, 10 King's College Road, Toronto, ON, M5S 3G4, Canada (email: jwsimpson@ece.utoronto.ca).

E. Farantatos, M. Patel, and A. Haddadi are with the Electric Power Research Institute, Palo Alto, CA 94304 USA (e-mail: efarantatos@epri.com; mpatel@epri.com; AHaddadi@epri.com).

This work was funded under EPRI Project #10009168: Wide-Area Hierarchical Frequency and Voltage Control for Next Generation Transmission Grids.

$\boldsymbol{Y}^k = [\Delta \boldsymbol{y}^{k-h+1}, \ldots, \Delta \boldsymbol{y}^k]^\top \in \mathbb{R}^{h \times n}$. Here and also in [1], we focus on maintaining voltage constraints at all buses and therefore assume all bus voltages are measured. This assumption can be relaxed by incorporating optimal PMU placement and state estimation approaches, but this is not our focus here.

B. Robust Estimation Method

Traditional least-squares estimates are highly sensitive to data outliers [4], which may occur in the collected data due to post-contingency voltage transients. To ensure reliable online estimation, we consider the fast robust multivariate regression method proposed in [4] to estimate the sensitivity matrix $\boldsymbol{\Pi}^k$ of (1) in a recursive manner. This method begins by generating k_n trials, each of which consists of $n+m+1$ samples that are randomly drawn from the sample data $\boldsymbol{Z}^k$. Let $(\boldsymbol{\mu}_{0,j}, \boldsymbol{\Sigma}_{0,j})$ be the start for the j^{th} trial with $\boldsymbol{\mu}_{0,j}$ and $\boldsymbol{\Sigma}_{0,j}$ being the sample mean and sample covariance matrix, respectively. Compute Mahalanobis distances $D_i(\boldsymbol{\mu}_{0,j}, \boldsymbol{\Sigma}_{0,j}) = \sqrt{(\boldsymbol{z}_i - \boldsymbol{\mu}_{0,j})\boldsymbol{\Sigma}_{0,j}^{-1}(\boldsymbol{z}_i - \boldsymbol{\mu}_{0,j})^\top}$ for all h samples with $\boldsymbol{z}_i$ being the i^{th} sample (row) of $\boldsymbol{Z}^k$. At the next iteration, the estimator $(\boldsymbol{\mu}_{1,j}, \boldsymbol{\Sigma}_{1,j})$ is computed from $c_n \approx h/2$ samples corresponding to the smallest Mahalanobis distances (used here to distinguish outliers). This iteration is continued for t steps with the estimator at the last step $(\boldsymbol{\mu}_{t,j}, \boldsymbol{\Sigma}_{t,j})$ being the attractor. The final estimate $\boldsymbol{\Sigma}$ is the one with the lowest determinant among all k_n attractors. More details including parameter settings of k_n and t can be found in [4].

Given the dataset $\boldsymbol{Z}^k$, the robust method (RM) returns

$$\{\boldsymbol{Z}^k\} \xrightarrow{RM} \{\boldsymbol{\Sigma}^k\} \tag{2}$$

where $\boldsymbol{\Sigma}^k \in \mathbb{R}^{(m+n)\times(m+n)}$ can be partitioned as

$$\boldsymbol{\Sigma}^k = \begin{bmatrix} \boldsymbol{\Sigma}_{uu}^k & \boldsymbol{\Sigma}_{uy}^k \\ \boldsymbol{\Sigma}_{yu}^k & \boldsymbol{\Sigma}_{yy}^k \end{bmatrix}.$$

The sensitivity matrix $\boldsymbol{\Pi}^k$ is then estimated by [5]

$$\boldsymbol{\Pi}^k = \left(\left(\boldsymbol{\Sigma}_{uu}^k\right)^{-1} \boldsymbol{\Sigma}_{uy}^k\right)^\top. \tag{3}$$

The successful estimation of (3) relies on the assumption that the sampling distribution of joint variables $(\Delta \boldsymbol{u}, \Delta \boldsymbol{y})$ in (1) follows a multivariate Gaussian distribution with $\boldsymbol{\Sigma}_{uu}$ being positive definite [5]. This assumption is always satisfied in power systems for two reasons: 1) the normal distribution serves as a bona fide population model of random power fluctuations [2], [6]; 2) the sampling distributions of many multivariate statistics are approximately normal regardless of the parent population, because of a central limit effect [7]. While the numerical stability of the matrix inverse in (3) is significantly affected by the highly correlated measurements, this problem can be effectively relieved by increasing the sampling rate and recording time or using the regularization technique [6].

C. Rolling Average for Sensitivity Smoothing

In practice, due to variations in nodal power injections (e.g., stochastic load variations), the estimated sensitivity model $\boldsymbol{\Pi}^k$ may fluctuate, even while the system operates around a steady state. To filter these unwanted noisy components during online operation, we employ the rolling average

$$\tilde{\boldsymbol{\Pi}}^k = \frac{1}{r}\sum_{i=1}^{r} \boldsymbol{\Pi}^{k-i+1} \tag{4}$$

where $\tilde{\boldsymbol{\Pi}}^k$ is the average of r consecutive samples. Note that the moving average and RM serve different functions: the former aims to smooth the variations of sensitivity model caused by *operating point fluctuations*, while the latter aims to minimize the bias introduced by *the outliers in the data*.

D. Event-Triggering for Reduced Computation

While during online operation it is desirable to continuously update $\boldsymbol{\Pi}^k$ based on the latest measurements, this increases computational burden. To this end, we consider an event-triggered sensitivity updating approach. When new measurements $(\Delta \boldsymbol{u}^{k+1}, \Delta \boldsymbol{y}^{k+1})$ are available, the predicted output $\Delta \hat{\boldsymbol{y}}^{k+1} = \tilde{\boldsymbol{\Pi}}^k \Delta \boldsymbol{u}^{k+1}$ is calculated based on the current model $\tilde{\boldsymbol{\Pi}}^k$ and compared with the new measured output $\Delta \boldsymbol{y}^{k+1}$. If the relative error $||\Delta \hat{\boldsymbol{y}}^{k+1} - \Delta \boldsymbol{y}^{k+1}||/||\Delta \boldsymbol{y}^{k+1}||$ is larger than a preset threshold δ, i.e., the current model presents a poor predictive performance due to changing system conditions, the calculation process (2)-(3) is activated to update the sensitivity model, otherwise, the same sensitivity model is used.

E. Parameter Tuning

There are three parameters to be tuned in the proposed method: the length of estimation window h, the length of moving average window r, and the preset threshold δ. Fortunately, these parameters are weakly correlated and can be tuned separately. The following rules can be used to determine the reasonable values for these parameters:

1) h is a compromise between computing efficiency and estimation accuracy; a value of h six times larger than the joint variable's dimension $n+m$ can guarantee the estimate accuracy [4];
2) r is a compromise between smoothing of the sensitivity estimate and response speed, but should not be selected too large to degrade the adaptation speed of RM;
3) The preset threshold δ defines the frequency of adaptation, so the smaller the preset threshold is, the more frequent the adaptation.

III. CASE STUDY

Fig. 1 shows the diagram of detailed one-area nonlinear power system model, which is built in [1] and adopted here for test purposes. Note that the proposed online controller is a supervisory controller, which acts by modifying the set-points of control devices. For convenience, we refer to the controller [1, Eq. (6)] with the fixed model-based sensitivity matrix as the *model-based controller*, while [1, Eq. (6)] with the sensitivity model updating process (1)-(4) described in Section II is the *model-free controller*.

During the simulation, Gaussian distributed random reactive power variations with zero mean are added to the power generation of the IBRs at buses 4 and 7; the standard deviations are both 1% of the respective IBR ratings. These power variations induce voltage changes at the terminals of the SGs and SVCs, activating the voltage control loops of these devices. This yields sufficient excitation across the system to

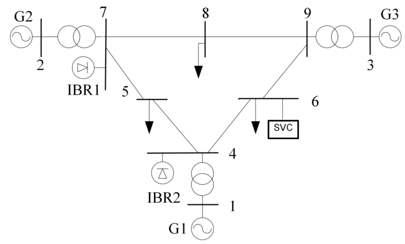

Figure 1: One-area test system.

ensure invertibility in (3), even when control commands are saturated at their limits. Additionally, as these voltage control loops are fast and of high gain, for simplicity the device set-point changes $\Delta \boldsymbol{u}$ are approximated by the measurements of corresponding device output variations (e.g., AVR voltage set-point change is approximated by the terminal voltage variation of SG). Measurement collection begins at $t = 0$s, with a sampling period of 0.1s. After $h = 80$ samples have been collected, a first estimate of $\boldsymbol{\Pi}^k$ is constructed and the controller is enabled at $t = 8$s. All measurements are corrupted by Gaussian noise with SNR approximately being 60 dB. Throughout we use a 10-sample rolling average window ($r = 10$). The other device and controller parameters used are the same as those in [1], unless specifically stated differently. Note that in the case studies that follow, the controller is enabled before the disturbance occurs and terminated after the system recovery from the disturbance, i.e., the proposed method is tested both in transient and steady states.

1) Scenario 1 – Basic effectiveness test

A 120 MVar reactive power disturbance occurs at bus 8 at $t = 10$s. To enourage IBR response, the weight matrices from [1] are selected as $\boldsymbol{R}_{\text{ibr}} = \boldsymbol{I}$, $\boldsymbol{R}_{\text{sg}} = \boldsymbol{R}_{\text{svc}} = 100\boldsymbol{I}$. Fig. 2 compares closed-loop responses obtained with the model-based controller and model-free controller. From Fig. 2, we observe that the model-free controller produces a closed-loop response which is almost identical to the model-based controller; this illustrates the basic effectiveness of the proposed modification.

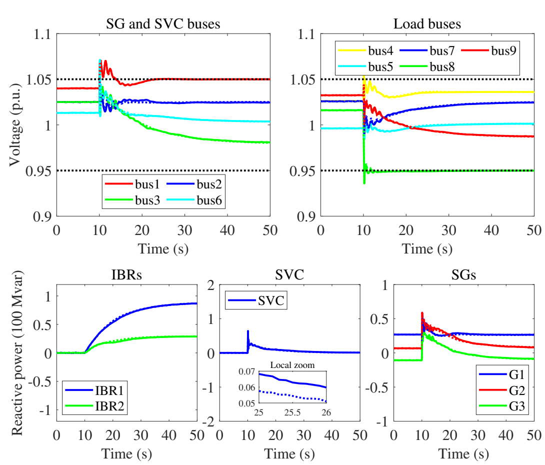

Figure 2: Voltage and reactive power profiles during disturbance (dotted: model-based, solid: model-free).

2) Scenario 2 – Model uncertainty test

We apply 40 MVar reactive power disturbance at bus 8 at $t = 10$s and trip the transmission line between buses 7 and 8 at the same time. To better highlight the impact of system topology change, the weight matrices from [1] are set as $\boldsymbol{R}_{\text{ibr}} = \boldsymbol{R}_{\text{svc}} = \boldsymbol{I}$, $\boldsymbol{R}_{\text{sg}} = 100\boldsymbol{I}$. We consider three control cases: the first is the model-free controller, the other two are the model-based controller with accurate and inaccurate sensitivity information, respectively, where the inaccurate sensitivity information is calculated based on the pre-line-trip system topology.

Fig. 3 shows the simulation results. The response with the model-based controller with inaccurate sensitivity information leads to persistent voltage violations at buses 7 and 8; see Scenario 7 of [1] for further explanation. In contrast, the model-based controller with accurate sensitivity information shows improved voltage regulation performance. The model-free controller adapts to the topology change, and converges towards the same steady-state that the model-based controller with accurate sensitivity information produces.

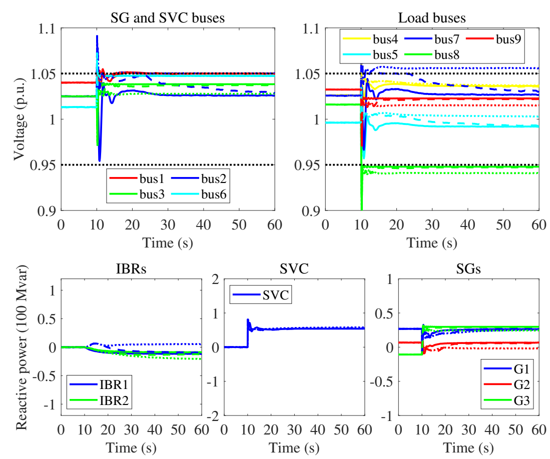

Figure 3: Voltage and reactive power profiles during disturbance (dotted: model-based (inaccurate), solid: model-based (accurate), dashed: model-free).

3) Scenario 3 – Regression method comparison

We next compare the estimation performance of the RM with two other popular regression methods: traditional ordinary least-squares (OLS) and partial least-squares (PLS) used in [2]. The disturbance is the same as in Scenario 2, but occurs at $t = 20$s. Fig. 4 shows the variation of element $\frac{\partial v_8}{\partial v_2}$ in $\boldsymbol{\Pi}$ that has the biggest change during disturbance. From Fig. 4, it is clear that OLS and PLS are sensitive to the outliers in the data collected during system dynamic transients after the contingency occurs, even when a significantly long data window length ($h = 120$) is applied. In contrast, the estimate produced by RM is not sensitive to these outlier data points, without any significant sacrifice in computation speed. From Fig. 4, we also observe that the sensitivity model varies even if the bias introduced by outliers have been minimized by RM ($r = 1$). This variation is caused by the operating point fluctuation and smoothed by the moving average ($r = 10$).

4) Scenario 4 – Event-trigger approach test

Finally, we test the addition of event-triggering as described in Section II-D; the disturbance is the same as in Scenario 2. Fig. 5 compares the control performance with and without event triggering. In this case, the event-triggered updating approach starts at $t = 10$s and ends at $t = 28$s with

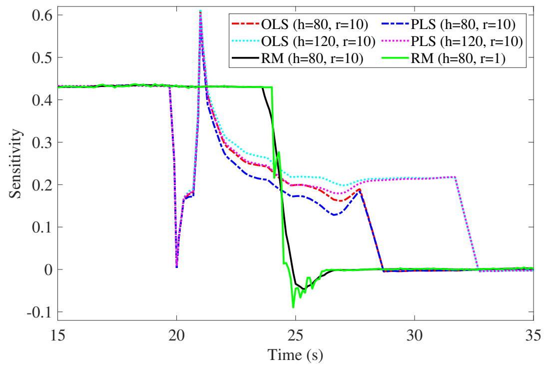

Figure 4: Element variation during disturbance

$\delta = 0.05$. Note that the actual time needed for the matrices to update is around 3 s (see Fig. 4). We observe that the event-triggered updating approach obtains almost the same control performance as that in continuous updating approach.

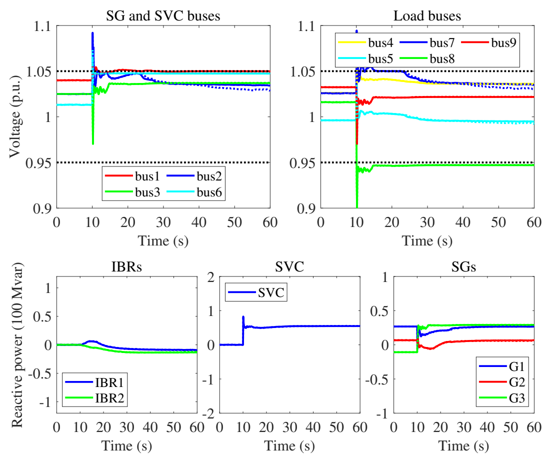

Figure 5: Voltage and reactive power profiles (dotted: continuous updating, solid: event-triggered updating).

IV. Conclusion

The voltage control scheme of [1] has been rendered model-free by integrating online sensitivity estimation via a robust regression technique. The proposed model-free approach provides an adaptive, robust, and efficient method of voltage control for next-generation transmission grids.

References

[1] Z. Tang, E. Ekomwenrenren, Simpson-Porco, *et al.*, "Measurement-based fast coordinated voltage control for transmission grids," *IEEE Transactions on Power Systems*, vol. 36, no. 4, pp. 3416–3429, 2021.

[2] S. Nowak, Y. C. Chen, and L. Wang, "Measurement-based optimal der dispatch with a recursively estimated sensitivity model," *IEEE Transactions on Power Systems*, vol. 35, no. 6, pp. 4792–4802, 2020.

[3] H. Xu, A. D. Domínguez-García, V. V. Veeravalli, and P. W. Sauer, "Data-driven voltage regulation in radial power distribution systems," *IEEE Transactions on Power Systems*, vol. 35, no. 3, pp. 2133–2143, 2020.

[4] D. J. Olive, "A resistant estimator of multivariate location and dispersion," *Computational statistics & data analysis*, vol. 46, no. 1, pp. 93–102, 2004.

[5] P. J. Rousseeuw, S. Van Aelst, K. Van Driessen, and J. A. Gulló, "Robust multivariate regression," *Technometrics*, vol. 46, no. 3, pp. 293–305, 2004.

[6] J. Zhang, Z. Wang, X. Zheng, *et al.*, "Locally weighted ridge regression for power system online sensitivity identification considering data collinearity," *IEEE Transactions on Power Systems*, vol. 33, no. 2, pp. 1624–1634, 2017.

[7] R. A. Johnson and D. W. Wichern, *Applied multivariate statistical analysis*, vol. 6. Pearson London, UK:, 2014.